Unfavorable Soil Environment for Root-Knot Nematode Infestation: Insights from Metabolomics and Microbial Diversity Analysis in Tomato Rhizosphere Soil

Jianqing Ma[1#], Weiping Zhang[4#], Yuanyuan Zhou[1], Jinrui Jing[1], Xuejin Yang[1], Xinyi Peng[1], Xiangdong Qin[2], Aimin Zhang[1,2,3], Gangyong Zhao[1,2,3], Dandan Cao[1,2,3*]**

[1]College of Life Science, Hebei University, Baoding, 071002, China
[2]Hebei Innovation Center for Bioengineering and Biotechnology, Hebei University, Baoding, 071002, China
[3]Engineering Research Center of Ecological Safety and Conservation in Beijing-Tianjin-Hebei (Xiong'an New Area) of MOE, Baoding, 071002, China
[4]Seed Workstation of the Agriculture and Rural Department of Ningxia Hui Autonomous Region, Yinchuan, 750000, China

Abstract

Plant root-knot disease caused by nematodes is a serious threat to agricultural production worldwide, second only to fungal diseases. *Meloidogyne incognita* is the most prevalent nematode species among RKN infested vegetables and cash crops. To explore the most potential biocontrol agents for *Meloidogyne incognita*, this study employed metabolomics and high-throughput sequencing approaches to assess alterations in metabolite profiles and microbial community structures of the rhizosphere soil around tomato (*Solanum lycopersicum)* roots before and after *Meloidogyne incognita* infestation. Subsequently, a comprehensive analysis of the metabolome and microbial diversity was conducted to identify differentially accumulated metabolites, microbes, and their correlation with each other. As a result, a total of 51 metabolites and 28 microbial genera exhibited significant differences in abundance between the treatments. Specifically, 27 metabolites were increased in concentration while 24 decreased, and the abundance of 25 bacterial genera and three fungal species was significantly altered. Further analysis revealed that five metabolites, including 5-fluorouridine monophosphate and fusarochromanone, as well as nine microbial genera, such as *Bacillus, Streptomyces,* and *Paenibacillus,* exhibited potential correlation with the biocontrol agents. In conclusion, the infestation of tomatoes by *M. incognita* results in substantial alterations to the metabolite profiles and microbial community

* e-mail: caodandan666@163.com
** e-mail: 18603220833@126.com
# equal contribution

structures within the rhizosphere soil. Five of the metabolites and nine microbial genera were identified as potential candidates for biocontrol of *M. incognita*.

Introduction

The root-knot nematodes (RKN) disease induced by *Meloidogyne* spp. was widespread and caused a significant economic impact on a global scale [1]. Among the numerous pathogens associated with RKN, *Meloidogyne incognita* is considered to be the most severe pathogeny. It could infect over 3000 plant species, including food crops, cash crops, vegetables, fruit trees, ornamental plants, and weeds [2]. The second-stage juveniles (J2s) of *M. incognita* predominantly initiate infection in plant roots. This phenomenon results in the impairment of the plant's nutrient assimilation capabilities, thereby impeding the growth and development of the aboveground parts, ultimately leading to stunted growth, premature senescence, and potentially complete desiccation and plant death.

The rhizosphere soil of plants is the main site for J2 activity and infection. The rhizosphere, which serves as the interface between plants and soil, is characterized by dense microbial communities and metabolites [3]. Plants utilize their root system to acquire nutrients and energy from the soil, facilitating their metabolic needs for their growth and development. On the other hand, the roots and exudates may attract a wide range of microorganisms in the rhizosphere by means of nutrient and mucilage secretion, among other aspects [4]. The root exudates of plants infested by *M. incognita* may be altered in composition, resulting in the attraction of a greater number of advantageous microbes. Scientific investigations have revealed that a range of compounds, such as coumarins, triterpenes, flavonoids, benzoxazinoids, phytohormones, and others, can stimulate or inhibit the proliferation of specific microbes that are in close proximity to the host plants [5-7]. Finkel et al. have demonstrated that *Variovorax* bacteria can regulate *Arabidopsis* root growth by influencing the levels of plant hormones auxin and ethylene [8]. Plenty of evidence is also present for the ability of plants to regulate their microbiome by the exudation of various metabolites, pointing to potentially reciprocal relationships between the microbiome and metabolome of the host plant [9]. Therefore, it is possible to propose isolating chemical compounds and microorganisms with biocontrol effects from rhizosphere soil.

Exploring new biocontrol factors from the rhizosphere micro-environment of plants is currently a hot topic in RKN biocontrol, as demonstrated by the extensive current research efforts [10, 11]. The microorganisms in the rhizosphere's soil directly or indirectly influence plant metabolism [9] and are a potential source for developing novel biocontrol agents against *M. incognita*. Research has shown that differences in microbial communities' composition and the abundance of functional genes and metabolites have been found in soils with high and low *M. incognita* infestation levels [12]. When *M. incognita* J2s infected tobacco, the relative abundance of certain rhizosphere bacterial genera and genes related to metabolic and signal transduction functions significantly increased [13]. Therefore, it is very feasible to screen biocontrol factors with potential by utilizing plant rhizosphere metabolomics and microbial diversity.

It can be observed that the presence of *M. incognita* in plants may alter the metabolite profiles and microbial community structures within the rhizosphere soil. Accordingly, the objective of this study was to identify the metabolites and microorganisms with potential control for RKN based on examining the alterations in the rhizosphere soil of tomato plants employing metabolomic profiling and high-throughput sequencing. The results will establish a theoretical basis for accelerating the implementation of innovative biocontrol practices and pesticides.

Materials and Methods

Experimental Materials

The initial *M. incognita* population was obtained from the Academy of Agriculture and Forestry Sciences of Beijing, China, and subsequently propagated using living tomato plants in a laboratory incubator. The Qinshu Shanghai 908 tomato cultivar, which was procured from Xi'an Qinshu Agriculture Company Limited, was used as the plant material in this study. The experiment was conducted in 2021 at the Agricultural Environmental Ecology Research Laboratory of Hebei Innovation Center for Bioengineering and Biotechnology of Hebei University, China (38°87' N,115°51' E).

Rhizosphere Soil Samples

Four tomato seeds were sown in each of the plastic pots, with dimensions of 11 cm in height and diameter, filled with 250 g of soil obtained from the Baoding urban area of Hebei Province, China. The soil contained 52.90 ± 0.22 mg/kg of total nitrogen, 16.44 ± 0.11 mg/kg of available phosphorus, 132.55 ± 1.29 mg/kg of total potassium, and 0.22 ± 0.01% organic matter. The tomato plants were grown in a controlled environment chamber specifically designed for climate simulation through
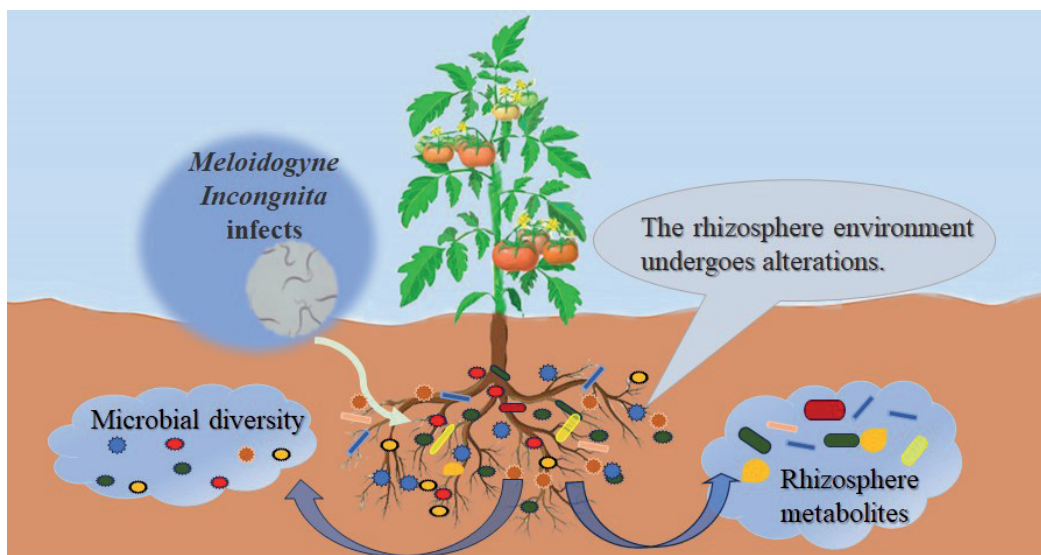
Fig. 1. Experimental mode diagram.

artificial intelligence. Inoculation with *M. incognita* was performed once the tomato seedlings had reached the 3-4 leaf stage. To introduce the nematodes, small holes were carefully created in the soil near the roots using a glass rod, and a suspension containing 2000 *M. incognita* J2s was then infused using a pipette. After a period of 35 days, soil samples (Nematode-infested Soil, NS) were collected from the rhizosphere-surrounding area. Rhizosphere soil of tomato plants without the presence of nematodes was also collected to be used as the control (Healthy Soil, HS) (Fig. 1). Three replicates were obtained for each soil sample. The samples were stored in a -80°C freezer for DNA and metabolite extraction (performed one week after sampling) and were sent to Shanghai Majorbio Bio-pharm Technology Co., Ltd. (China) for metabolomics and high-throughput DNA sequencing.

Metabolomics Analysis

Soil samples weighing 50 mg were accurately measured and subjected to metabolite extraction using a methanol: water (4:1, v/v) solution at a volume of 400 µL. The resulting soil suspension was allowed to settle at a temperature of -20 °C and subsequently processed using a high-throughput tissue grinder, Wonbio-96c (Shanghai Wanbo Biotechnology Co., Ltd), at a frequency of 50 Hz for 6 minutes. This was followed by vortexing for 30 seconds and ultrasonication at a frequency of 40 kHz for 30 minutes at a temperature of

5 °C. To precipitate proteins, the samples were placed at -20 °C for 30 minutes. Subsequently, centrifugation was performed at 13000 g and 4 °C for 15 minutes, and the resulting supernatant was carefully transferred to sample vials for LC-MS/MS analysis. After UPLC-TOF/MS analyses, the raw data were imported into Progenesis QI 2.3 (Nonlinear Dynamics, Waters, USA) for peak detection and alignment. The mass spectra features were identified by querying the accurate mass, MS/MS fragment spectra, and isotope ratio difference information in reliable biochemical databases such as the Human Metabolome Database (HMDB) (http://www.hmdb.ca/) and Metlin Database (https://metlin.scripps.edu/). Principle Component Analysis (PCA) was employed to comprehensively characterize the metabolic data, enabling visualization of treatment clustering, trends, and outliers. Orthogonal partial least squares discriminate analysis (OPLS-DA) was utilized for statistical analysis to identify global metabolic alterations between the different treatment groups. Univariate analysis (T-test) was employed to identify differential metabolites between the groups.

High-Throughput DNA Sequencing

The total DNA of the microbial communities in the soil samples was extracted using a DNA extraction kit (E.Z.N.A ® Soil DNA Kit). The purity, concentration, and integrity of the extracted DNA were assessed using a microspectrophotometer and 1% agarose gel

Table 1. Primers used for PCR amplification.

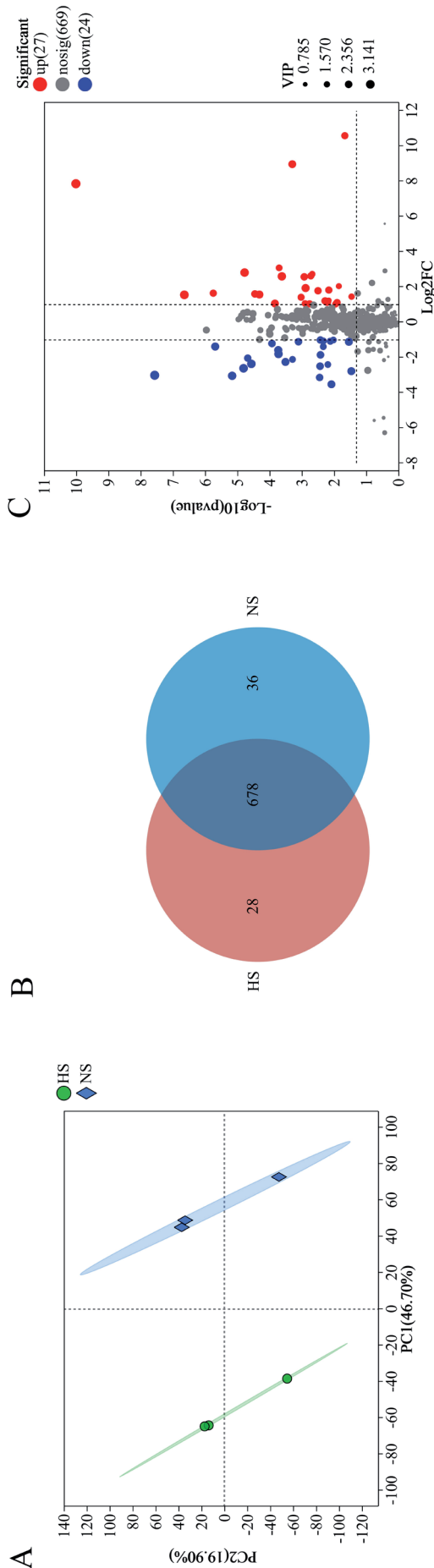| Name	Forward primer sequence (5'-3')	Reverse primer sequence (5'-3')
Bacterial 16s region	ACTCCTACGGGAGGCAGCAG	GGACTACHVGGGTWTCTAAT
Fungal ITS1 region	CTTGGTCATTTAGAGGAAGTAA	GCTGCGTTCTTCATCGATGC

Fig. 2. Differential metabolite analysis in healthy soil (HS) and infested soil (NS). (A) Principal component analysis (PCA) score plots; (B) Venn diagram of total metabolites; (C) Volcano plot.

electrophoresis (voltage 5 V/cm, time 20 min). Primers 338F/806R and ITS1F/ITS2R (Table 1) were used to amplify the V3 to V4 variable regions of the bacterial 16S rRNA gene and the ITS1 region in fungi, respectively. The 16S rRNA gene PCR amplification was performed as follows: 95 ℃ for 3 min, 27 cycles (95 ℃ denaturation for 30 s, 55 ℃ annealing for 30 s, 72 ℃ extension for 30 s), final extension at 72 ℃ for 10 min, and a hold step at 4 ℃ (PCR instrument: ABI GeneAmp ® 9700 type). The PCR mixture contained 5 × TransStart FastPfu buffer 4 μL, 2.5 mM dNTPs 2 μL, forward primer (5 μM) 0.8 μL, reverse primer (5 μM) 0.8 μL, TransStart FastPfu DNA Polymerase 0.4 μL, template DNA 10 ng, and ddH$_2$O up to 20 μL. PCR reactions were performed in triplicate. The PCR product was extracted from 2% agarose gel and purified using the AxyPrep DNA Gel Extraction Kit (Axygen Biosciences, Union City, CA, USA) according to the manufacturer's instructions and quantified using a Quantus™ Fluorometer (Promega, USA).

The original amplicon sequences were processed and filtered with Fastp software (version 0.19.6) and Flash software (version 1.2.11) to obtain the final high-quality sequences. Duplicate sequences were removed using Uparse software (version 7.0.1090). The identified non-repetitive sequences were assigned to operational taxonomic units (OTUs) based on 97% similarity. Chimeras were removed, and the sequence with the highest abundance in each OTU was selected as a representative sequence of that OTU for subsequent bioinformatics analysis.

Microbial Community and Differential Abundance Analysis

OTUs were normalized based on the minimum sum count across the given OTU. The taxonomic annotation of each sequence was performed by alignment against the Silva 16S rRNA database using the RDP classifier software (version 2.11), with an alignment threshold of 70% to identify the microbial community composition of each sample at the phylum and genus levels, respectively. The alpha diversity metrics Chao index, which reflects community richness, and the Shannon index, which reflects community diversity, were calculated using Mothur software (version 1.30.2). Beta diversity analysis was performed using R language (version 3.3.1). Bray Curtis distances were calculated for the distance matrix, and PCoA was used to visually display the results. The stats package in the R language and the SciPy package in Python were used for the analysis of microbial community composition and the different abundances of different taxonomic groups.

Data Analysis

The SciPy (Python) software (Version 1.0.0) was employed to examine the association between differential metabolites and microbial diversity in soil samples. To

compare the mean values between groups, T-tests and one-way analysis of variance were conducted using the SPSS software, and Tukey's HSD method was employed for statistical significance testing at a significant level of 0.05 [14].

Results

Differentially Accumulated Metabolites of Rhizospheric Soils

The unsupervised principal component analysis (PCA) was employed to elucidate the metabolite differences between samples, with PC1 and PC2 accounting for 46.70% and 19.90% of the variance, respectively. A significant difference was observed in the total metabolite composition of the individual samples from the two groups based on their distribution across the PC axes. Notably, the individual samples from each treatment group, corresponding to the metabolite profiles from the rhizospheric soils before and after *M. incognita* infestation, were clustered (Fig. 2A). Venn analysis of the metabolites in healthy and infested soil, which numbered 706 and 714, respectively, revealed that 678 metabolites were shared between the two conditions. Additionally, 28 metabolites were unique to healthy soil, while 36 were exclusive to infested soil (Fig. 2B). A volcano plot was generated based on T-tests, where significant differentially accumulated metabolites were defined as having a VIP score > 1, a P-value < 0.05, and 0.5<fold change<2 (Fig. 2C). The volcano plot analysis revealed that 51 metabolites exhibited significant differential accumulation, while 27 metabolites were upregulated (Table 2) and 24 metabolites were downregulated (Table 3).

Differences in Microbial Community Composition

Following the optimization of the original bacterial sequences, a total of 296,094 sequences were obtained, with an average sequence length of 417.24 base pairs (bp). A total of 29,560 OUTs were obtained through cluster analysis, with species annotated to 39 phyla, 102 orders, 2,480 families, 688 genera, and 1,299 species. The original fungal sequence was optimized to yield a total of 356,980 sequences, with an average sequence length of 260.90 bp. Cluster analysis yielded 518 OUTs. The species were annotated to 7 phyla, 26 orders, 62 families, 208 genera, and 329 species.

Regarding the alpha diversity analysis, as shown in Table 4, the Shannon index of the bacterial community in healthy soil was comparatively greater than in infested soil. Conversely, the Shannon index of the fungal community of the healthy soil was comparatively lower than that of the infested soil. These results suggest variability in the richness and diversity of microorganisms between healthy and nematode-infested

soils, although none of the differences were statistically significant.

PCA revealed a clear distinction in the composition of bacterial and fungal communities in the soil samples of each treatment group, with the differences between the treatments being significantly greater than those within the soil samples from the same treatment (Fig. 3A-B). These results indicated that the beta diversity of the bacterial and fungal communities was significantly different between soils infested with *M. incognita* and healthy soils.

Assessing the differences in bacterial community structure and composition between healthy and infested soils at the phylum level, using a relative abundance greater than 1% as the threshold, revealed that the bacterial microbial community composition in the two soil treatment groups was similar (Fig. 4A), both containing 13 bacterial phyla. Among them, *Proteobacteria*, *Actinobacteriota*, *Firmicutes*, *Chioroidota,* and *Acidobacteriota* were the dominant bacterial phyla in the samples of each treatment group. *Proteobacteria* had a relative abundance of 30.07% in the healthy soils, which was higher compared to the 25.31% observed in the infested soils. *Actinobacteriota* had a relative abundance of 25.31% in infested soils, higher than 23.98% in healthy soils. *Firmicutes* had a relative abundance of 12.30% and 11.47% in healthy and infested soils, respectively. At the genus level, with a threshold of relative abundance not less than 1%, 28 bacterial genera were identified in both treatment groups (Fig. 4B). Among them, *Arthrobacter*, *Tumebacter*, and *Fictibacillus* were the dominant bacterial genera in both treatment groups. *Arthrobacter* had a relative abundance of 17.83% in the infested soils, higher compared to the 10.68% in the healthy soils. *Tumebacter* had a relative abundance of 4.42% in the healthy soils, higher compared to the 2.98% in the infested soils. *Fictibacillus* had a relative abundance of 4.22% and 2.79% in healthy and infested soils, respectively.

Using a relative abundance greater than 1% as the threshold, twenty-five bacterial genera exhibited significant differences in relative abundance (p < 0.05) between the two soil treatment groups (Fig. 5). The relative abundances of 11 bacterial genera were higher in NS than that in HS, as follows: *Arthrobacter, norank_f__Vicinamibacteraceae, Bacillus, Methylibium, norank_f__norank_o__ Vicinamibacterales, norank_f__norank_o__ SBR1031, Haliangium, Paenibacillus, Streptomyces, and norank_f__norank_o__norank_c_KD4-96, norank_f__Anaerolineaceae*. The relative abundance of these 11 bacterial genera was 1.67, 2.10, 1.80, 2.39, 3.59, 2.22, 1.71, 1.55, 2.46, 3.51, and 3.12 times higher in NS than that in HS, respectively. A total of 14 bacterial genera exhibited a higher relative abundance in HS compared to NS, as follows: *Tumebacillus, Fictibacillus, Massilia, Microvirga, Nocardioides, Marmoricola, Herpetosiphon, Sphingomonas, Rubellimicrobium, unclassified_f__Comamonadaceae, norank_f__*

Table 2. The significantly upregulated metabolites in rhizosphere soil after M. incognita infestation.

Metabolite	Formula	VIP	FC(NS/HS)	*P*_value
6-Dehydrotestosterone glucuronide	$C_{25}H_{34}O_8$	2.0789	1540.1886	0.02171
3,4-Dimethyl-5-pentyl-2-furanoctanoic acid	$C_{19}H_{32}O_3$	2.0663	502.4501	0.0005086
1-(3-Methoxy-4-hydroxy)-phenyl-6,7-dihydroxy-isochroman	$C_{16}H_{16}O_5$	3.4489	232.9916	9.76E-11
Cysteinyl-Hydroxyproline	$C_8H_{14}N_2O_4S$	1.8089	8.5062	0.0001984
Spirotaccagenin	$C_{27}H_{42}O_5$	2.966	7.0668	1.68E-05
3-Deoxyguanosine	$C_{10}H_{13}N_5O_4$	1.341	6.6519	0.002111
Kudzusaponin SA4	$C_{47}H_{74}O_{20}$	1.6525	6.1854	0.001908
Daphniphylline	$C_{32}H_{49}NO_5$	2.3862	6.0933	0.0002412
5'-Methylthioadenosine	$C_{11}H_{15}N_5O_3S$	2.2195	5.9738	0.001193
Deoxycytidine	$C_9H_{13}N_3O_4$	1.3782	4.1377	0.01415
Anhydroamarouciaxanthin B	$C_{40}H_{50}O_3$	2.2079	3.8417	0.001314
9,10,16-trihydroxy palmitic acid	$C_{16}H_{32}O_5$	2.0967	3.5518	0.006907
3b-Allotetrahydrocortisol	$C_{21}H_{34}O_5$	2.2103	3.4563	0.003188
Glutamylserine	$C_8H_{14}N_2O_6$	2.1067	3.1398	1.79E-06
Deoxyguanosine	$C_{10}H_{13}N_5O_4$	2.246	3.0516	3.52E-05
(R)-3-Hydroxybutyric acid	$C_4H_8O_3$	2.1714	2.9772	4.85E-05
(3beta,17alpha,23R)-17,23-Epoxy-3,29-dihydroxy-27-norlanost-8-ene-15,24-dione	$C_{29}H_{44}O_5$	3.1664	2.9409	2.27E-07
Prostaglandin A1 ethyl ester	$C_{22}H_{36}O_4$	1.2947	2.7404	0.03517
Indole-3-carboxylic acid	$C_9H_7NO_2$	1.6598	2.674	0.0009537
N6-Methyl-2'-deoxyadenosine	$C_{11}H_{15}N_5O_3$	1.2571	2.3628	0.006875
LysoPC (20:3(5Z,8Z,11Z))	$C_{28}H_{52}NO_7P$	1.866	2.3161	0.005299
1-AG	$C_{23}H_{38}O_4$	2.8262	2.2365	0.006136
4-{[3-(hydroxymethyl)-3-methyloxiran-2-yl] methoxy}-7H-furo[3,2-g] chromen-7-one	$C_{16}H_{14}O_6$	2.1571	2.1662	0.01248
Hypoxanthine	$C_5H_4N_4O$	1.8006	2.0907	0.001265
11-Hydroxy-D4-neuroprostane	$C_{22}H_{32}O_5$	2.5643	2.0896	0.0001471
11-Oxohexadecanoic acid	$C_{16}H_{30}O_3$	2.1254	2.0624	0.001743
Auberganol	$C_{15}H_{28}O_2$	1.8219	2.0429	0.01122

Note: VIP indicates the VIP value of each metabolite in the OPLS-DA model between the two treatment groups. FC indicates the fold change of each metabolite concentration between the two groups. P_ value represents the significance test result of the difference between the two groups for that metabolite. The same applies in the table below.

Microscillaceae, Lechevalieria, norank_f__ norank_o__norank_c__norank_p__Armatimonadota, Pseudonocardia. The relative abundance of these 14 bacterial genera in HS was 1.53, 1.51, 3.41, 1.80, 2.79, 2.69, 5.19, 1.33, 2.27, 1.37, 1.93, 3.07, 2.37, and 4.66 times higher than that of NS, respectively.

Regarding the differences in the fungal community composition between healthy and infested soils at the phylum level, using a relative abundance greater than 1% as the threshold, a high similarity in the fungal microbial community between soil treatment groups was observed (Fig. 6A). Three fungal phyla, Ascomycota, unclassified_ k_ fungi, and Mortierellomycota, exhibited the highest relative abundance in both groups. Among them, Ascomycota was the most dominant fungal phylum in both samples, accounting for 98.03% and 90.75% of the total fungal community in healthy and infested soils, respectively. At the genus level, using a threshold of relative abundance greater than 1%, 14 fungal genera were identified in both soil treatment groups (Fig. 6B). *Iodophanus* was the dominant fungal genera in the samples of each treatment group. It had a

Table 3. The significantly downregulated metabolites in rhizosphere soil after M. incognita infestation.

Metabolite	Formula	VIP	FC(NS/HS)	*P*_value
Corchoroside B	$C_{29}H_{42}O_8$	2.0461	0.0872	0.008336
Eremopetasinorone A	$C_{13}H_{18}O_2$	1.828	0.114	0.003587
APC	$C_{33}H_{38}N_4O_8$	2.3515	0.1218	6.91E-06
Hordatine A glucoside	$C_{34}H_{48}N_8O_{10}$	2.7889	0.1244	2.72E-08
5-Fluorouridine monophosphate	$C_9H_{12}FN_2O_9P$	2.5413	0.1463	0.03454
Naphthalene-1,2-diol	$C_{10}H_8O_2$	3.0098	0.1636	1.56E-05
Mangostanol	$C_{24}H_{26}O_7$	1.9208	0.1778	0.003699
Tetranor-12(R)-HETE	$C_{16}H_{26}O_3$	1.4311	0.1897	0.006446
Glycyrrhizaflavonol A	$C_{20}H_{18}O_7$	2.949	0.1948	2.72E-05
Osmanthuside B	$C_{29}H_{36}O_{13}$	2.1319	0.2099	0.0003118
(2S,2'S)-Pyrosaccharopine	$C_{11}H_{18}N_2O_5$	1.771	0.2321	0.0005167
5-hydroxy-8-(2-hydroxypropan-2-yl)-4-propyl-2H,8H,9H-furo[2,3-h] chromen-2-one	$C_{17}H_{20}O_5$	2.1847	0.2441	2.10E-05
(6E,8R,10Z)-8-hydroxy-3-oxohexadecadienoic acid	$C_{16}H_{26}O_4$	1.9152	0.2773	0.003804
Alpinetin methyl ether	$C_{17}H_{16}O_4$	2.869	0.2874	0.0001893
Licochalcone A	$C_{21}H_{22}O_4$	2.2018	0.3343	0.0001861
Dopamine 4-sulfate	$C_8H_{11}NO_5S$	1.5108	0.3836	0.004648
Lycopersiconol	$C_{21}H_{34}O_3$	2.637	0.3852	2.06E-06
Carboxy-ibuprofen	$C_{13}H_{16}O_4$	2.2525	0.434	0.0001189
1-(9Z-hexadecenoyl)-glycero-3-phosphate	$C_{19}H_{37}O_7P$	2.1407	0.4645	0.02895
Traumatin	$C_{12}H_{20}O_3$	1.857	0.4656	0.0007893
Fusarochromanone	$C_{15}H_{20}N_2O_4$	1.9853	0.475	0.00768
Phenylglucuronide	$C_{12}H_{14}O_7$	2.0455	0.4775	0.004622
Tryptophyl-Lysine	$C_{17}H_{24}N_4O_3$	1.8446	0.4975	0.00378
Alisol A	$C_{30}H_{50}O_5$	1.4689	0.4977	0.009541

relative abundance of 56.92% in the healthy soils, higher compared to the 23.61% in the infested soils.

Using a relative abundance greater than 1% as the threshold, three fungal genera exhibited statistically significant differences (P < 0.05) (Fig. 7). Among them, there were two fungal genera; the relative abundance in NS was significantly higher than in HS, as follows: *unclassified_k__Fungi* and *Stachybotrys*. The relative abundance of these two fungal genera was 35.59 and 32.64 times higher in NS than that in HS, respectively. There was one fungal genus, *Iodophanus*, with a relative abundance of 56.92% in HS, significantly higher than in NS.

Correlation Analysis

In the correlation heat map between the 51 differential metabolites (27 upregulated and 24

Table 4. Alpha diversity of the bacterial and fungal communities in healthy soils (HS) and infested soils (NS).

Soil sample	Bacteria	Fungi
	Shannon index	Shannon index
HS	5.73±0.08a	1.9±0.08a
NS	5.66±0.05a	2.46±0.27a

Note: Different lowercase letters in the same column indicate significant differences between soil samples at P<0.05.

A

B

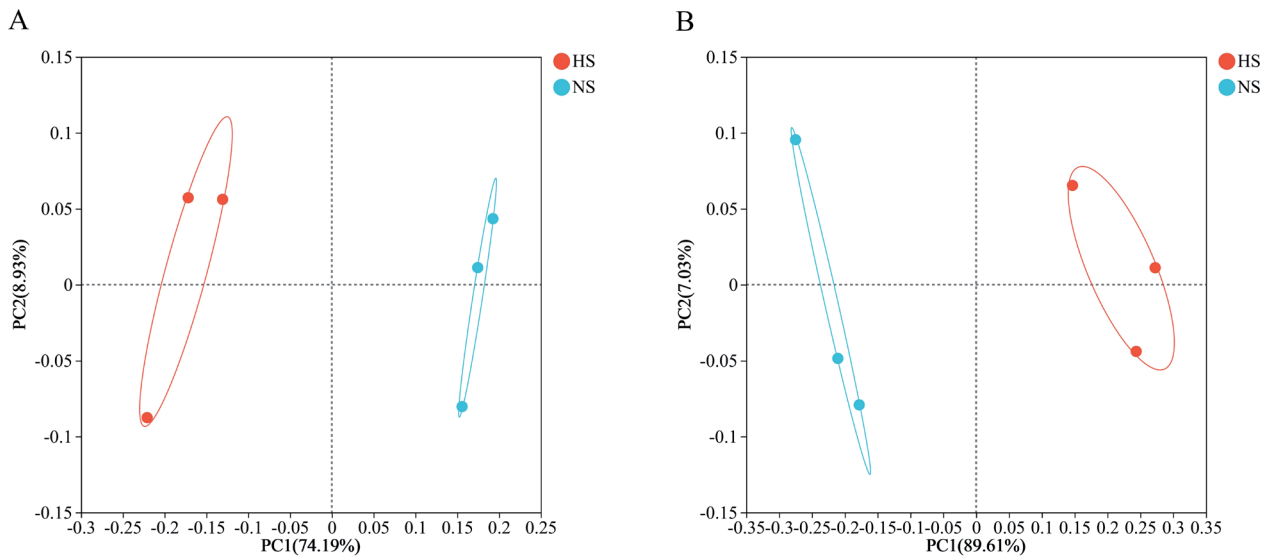

Fig. 3. PCA plot of beta diversity of the bacterial and fungal communities in healthy soils (HS) and infested soils (NS). (A) Bacteria. (B) Fungi.
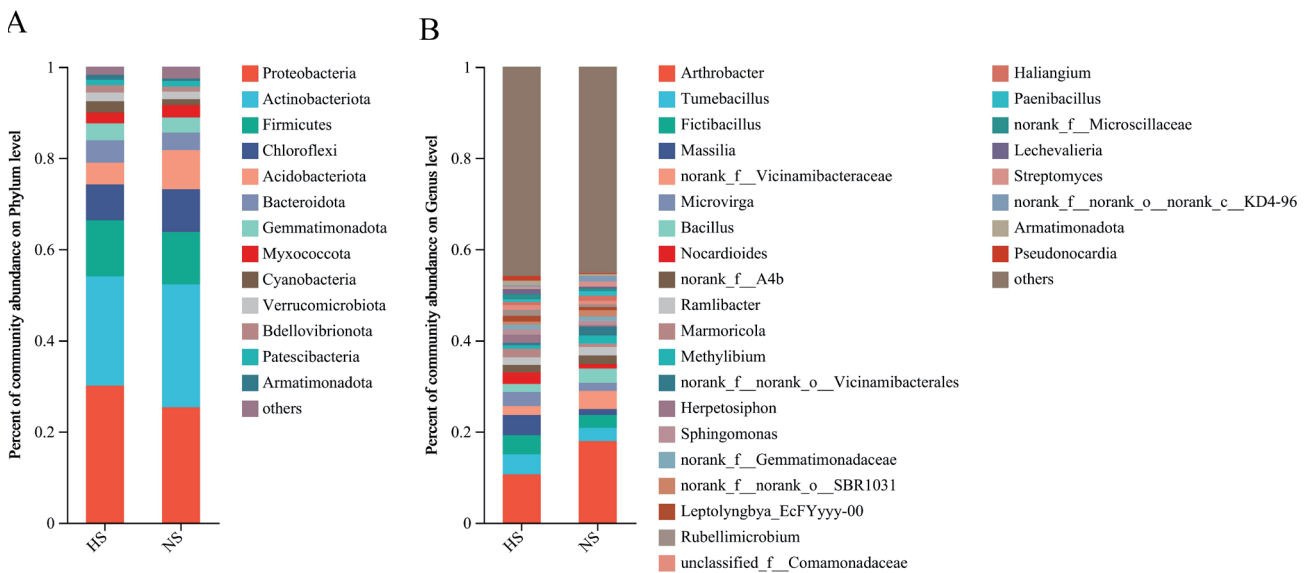
A

B

Fig. 4. Bacterial community composition in healthy soils (HS) and infested soils (NS). (A) Phylum. (B) Genus.

downregulated) and the 28 differential microbial genera (25 bacterial genera and three fungal genera) in the soils before and after infestation with *M. incognita* (Fig. 8), a total of 182 significant pairwise correlations were identified (P < 0.01, |r| > 0.9). These correlations included 49 metabolites and all microbial genera included in the analysis. Among them, five metabolites were associated with more microorganisms; they were eremopetasinolone A, fusarochromanone, auberganol, 5-fluorouridine monophosphate, and (2S, 2'S)-pyrosacharpine, respectively. Nine microbial genera are associated with more metabolites; they were *norank_f__ norank_o__norank_c__norank_p__Armatimonadota*, *Methylibium*, *Paenibacillus*, *Iodophanus*, *Haliangium*

Bacillus norank_f_Microscillaceae, *Streptomyces*, and *Marmoricola*, respectively.

Discussion

The current study aimed to discern the changes in the metabolite profiles among diverse soil samples attributed to *M. incognita* infestation in plants. Subsequently, following a correlation analysis between microbial genera and soil metabolites, we identified five metabolites that were significantly correlated with the abundance of specific microbial genera. Including 5-fluorouridine monophosphate, fusarochromanone,
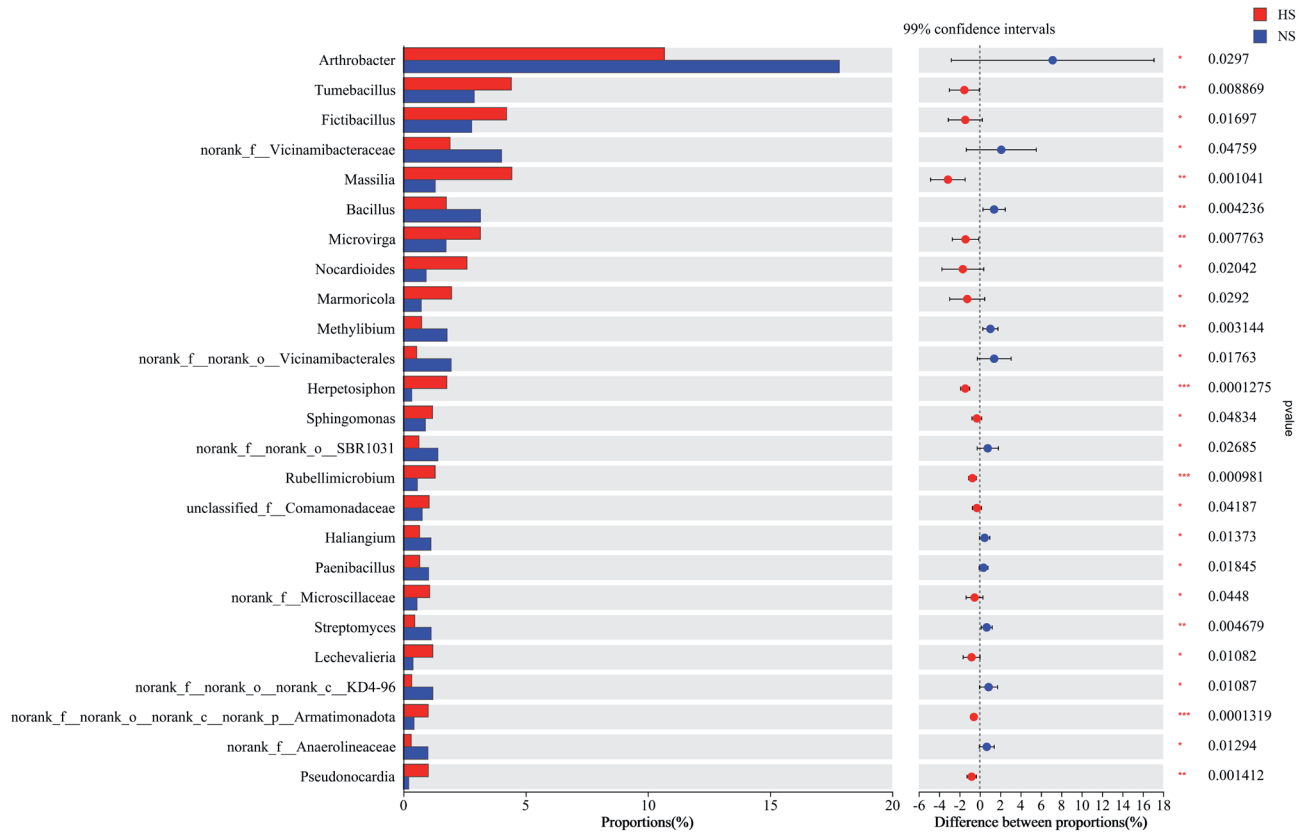
Fig. 5. Bacterial genera with significantly different abundance between healthy soils (HS) and infested soils (NS).
Note: The x-axis represents the average relative abundance of a species in different treatment groups, and the y-axis represents the different groups. *$P \leq .05$. **$P \leq .01$. ***$P \leq .001$.
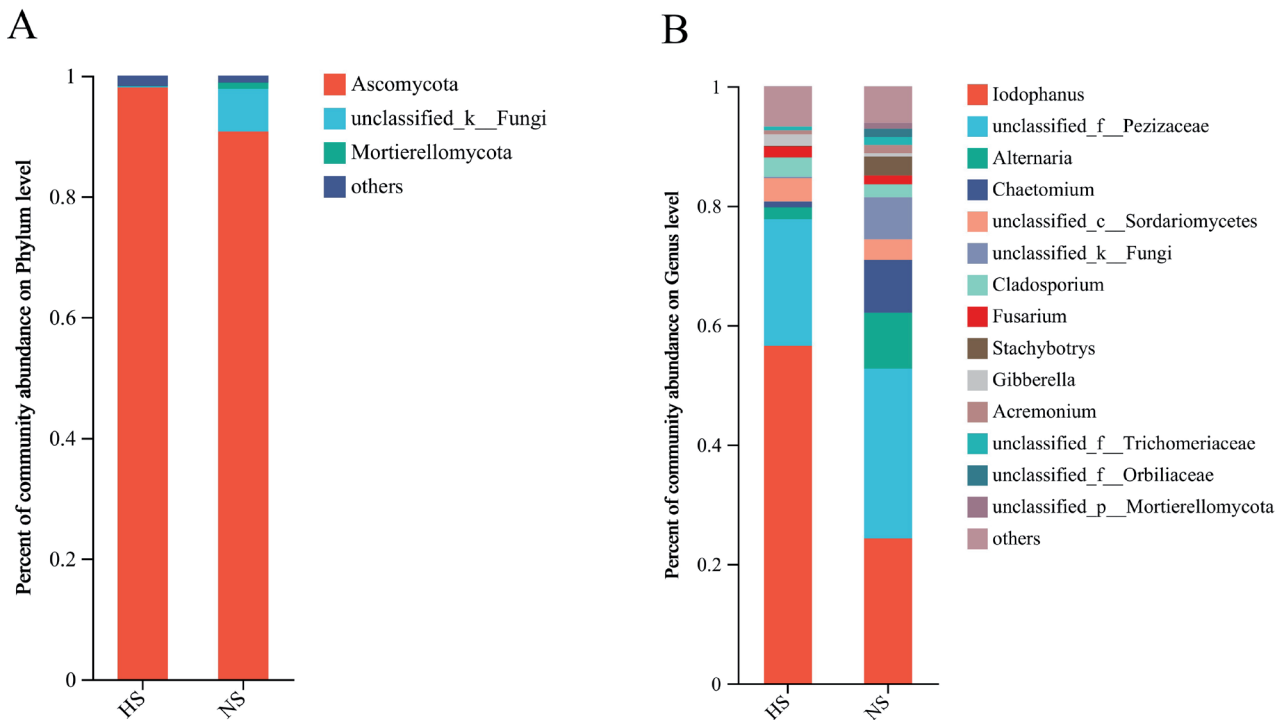

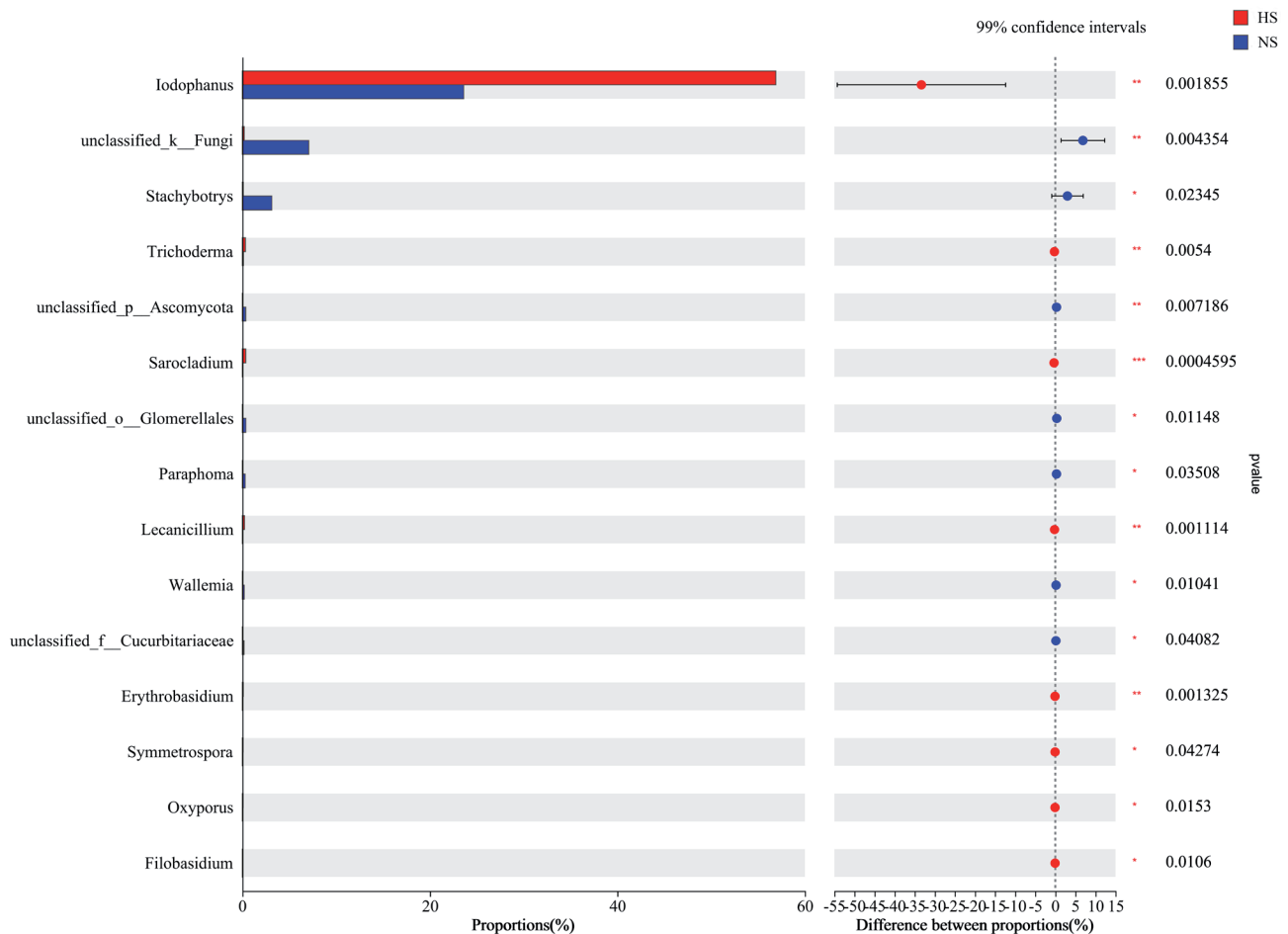Fig. 6. Fungal community composition in healthy soils (HS) and infested soils (NS). (A) Phylum. (B) Genus.

Fig. 7. Fungal genera with significantly different abundance between healthy soils (HS) and infested soils (NS).
Note: Same as Fig. 5.

eremopetasinolone A, auberganol, and (2S, 2'S)-pyrosaccharopine. According to Tables 2 and 3, except for auberganol, all metabolites were significantly upregulated after infection with *M. incognita*. The compound 5-fluorouridine has been identified as a specific antivirulence agent, which can disrupt bacterial RNA metabolism and inhibit the synthesis of pyridoxine, a key toxin, thereby reducing *Pseudomonas aeruginosa* virulence in *Caenorhabditis elegans* [15]. Additionally, 5-fluorouridine monophosphate may have potential therapeutic properties and application potential for treating *Candida albicans* infections [16]. Fusarochromanone is a poisonous metabolite generated by *Fusarium equiseti*, a fungus commonly found in the decomposing tissues of cereal plants in northern latitudes. As shown in previous studies, fusarochromanone serves as an adjuvant molecule, effectively impeding melanoma growth and recurrence by increasing tumor cell apoptosis and reducing tumor growth *in vivo* [17]. However, the potential impact of fusarochromanone on *M. incognita* fitness and metabolism remains unclear and warrants further investigation. Notably, the properties and effects of

eremopetasinolone A, auberganol, and (2S, 2'S)-pyrosaccharopine are not yet investigated.

It is crucial to acknowledge that rhizosphere soil metabolites are not solely derived from rhizosphere microorganisms. The role of root secretions in metabolite production should not be underestimated. According to reports, the root exudates of rosemary and marjoram can inhibit the survival, development, and reproduction of nematodes [18]. Therefore, metabolites with a weak correlation with changes in rhizosphere soil microbial communities in this study may be produced in plants. However, further exploration is needed to determine whether these metabolites have biocontrol potential.

The microbiome of the plant rhizosphere directly influences plant health and resistance to pathogens [19]. Following exposure to aboveground or belowground stressors, significant alterations in root metabolic profiles and gene expression occur in conjunction with changes to the rhizosphere microbial community [20]. In this study, we explore the differences in microbial community structures of the rhizosphere soil around tomato roots before and after *M. incognita* infestation. There were 51 microbial genera with significant differences. Among them, the relative abundance of 13
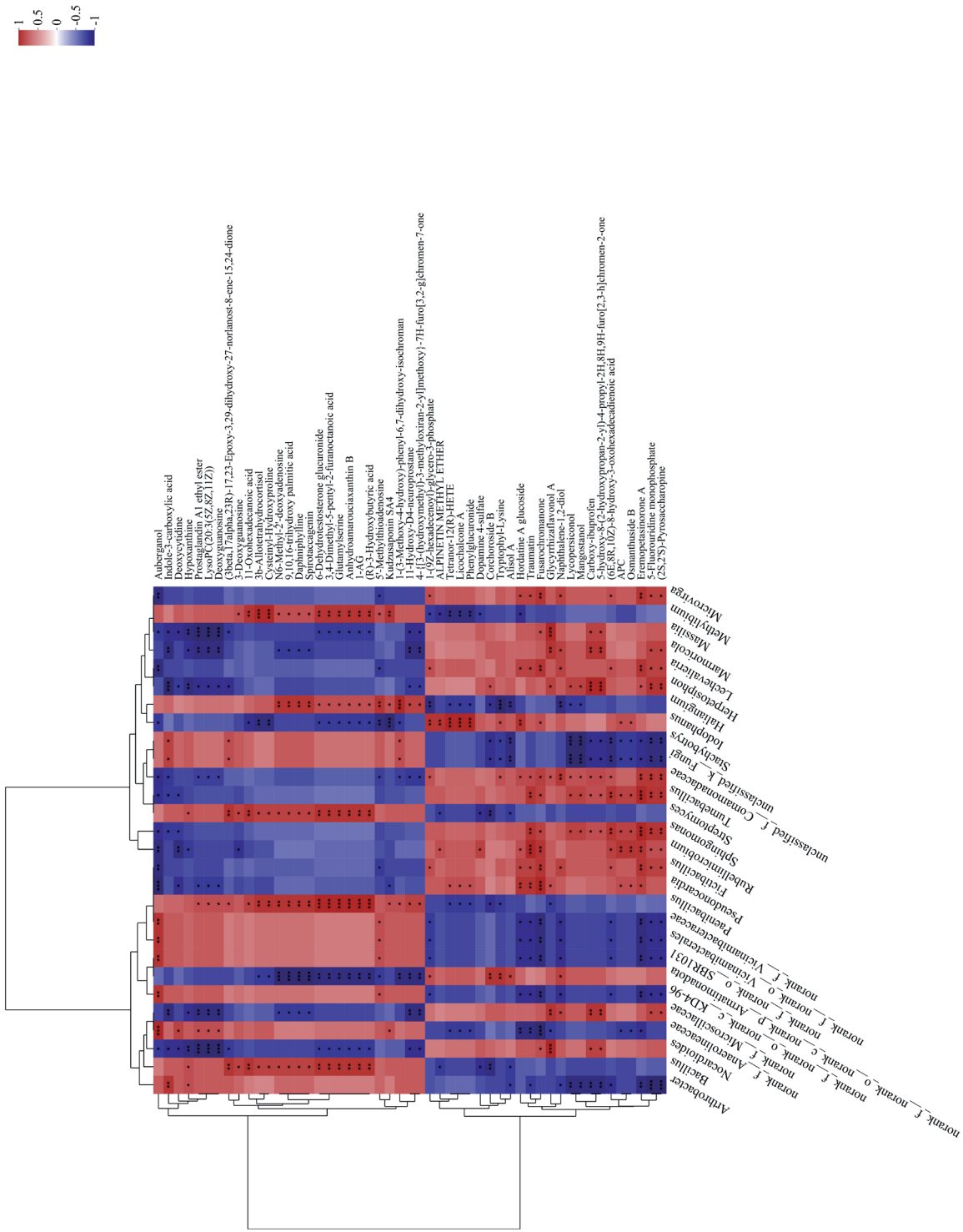
Fig. 8. Correlation Heatmap between the differentially accumulated metabolites and the differentially abundant microorganisms.

Note: The right side of the plot indicates the metabolite name, and the bottom indicates the microbial genera. Each lattice in the plot represents the correlation between two attributes (metabolite and microbial genus), and different colors represent the magnitude of the correlation coefficient between attributes.

*$P \leq .05$. **$P \leq .01$. ***$P \leq .001$.

microbial genera was significantly higher in NS than in HS. Previous research has established *Bacillus* as a well-established microorganism that can effectively inhibit the activity of *M. incognita*. *Bacillus*, a genus of bacteria that resides extracellularly between the rhizosphere and root cortex cells, has been classified as a rhizosphere bacterium that promotes plant growth and primarily protects against *M. incognita* through the secretion of hydrolases and secondary metabolites [21]. In a previous study, *Bacillus* strain R2, isolated from tomato, was highly effective against *M. incognita*, with a biocontrol lethality rate of 90.94%. Additionally, a nematocidal compound identified as styrene was isolated [22]. Notable antibiotics produced by *Streptomyces* include avermectin, meliloticin, and nicomycin, among others. According to reports, natural fermentation products contain eight avermectins with structurally similar properties and a common mother nucleus, each exhibiting insecticidal activity. The widely used ivermectins are highly effective antibiotics developed through structural modification of avermectins [23]. *Stachybotrys* exhibited nematicidal activity, up to 35% [24]. A significantly higher relative abundance of Methylibiumv has been reported in soil from artificially disturbed areas compared to naturally undisturbed areas [25]. It has been reported that *Haliangium* is isolated from coastal areas and confirmed to have salt tolerance properties [26]. *Paenibacillus* has been proven to have radiation resistance [27]. However, we observed that the relative abundance of 15 microbial genera was significantly higher in HS than in NS. *Fibribacillus phophorivorans* G25-29 has been proven to have nematicidal ability and can inhibit its free activity [28]. Two strains of bacteria with nematicidal ability have been isolated from mangrove sediments and identified as *Pseudonocardia* [29]. *Marmoricola* is an actinomycete found in oceans and ash, among other environments [30, 31].

Furthermore, nine microbial genera were identified as significantly associated with specific microorganisms through association analysis. Based on existing research results, among these nine microbial genera, *Bacillus* and *Streptomyces* have nematicidal activity. While *Paenibacillus*, *Methlibium*, *Halangium*, and *Marmoricola* were shown to be sensitive to abiotic stress conditions. However, no studies on *Iodophanus* and two other undefined bacterial genera have been conducted so far.

Conclusion

The presence of *M. incognita* in the rhizosphere soil of tomato plants has been observed to significantly impact the soil metabolite levels and microbial diversity. Through correlation analysis, a total of five metabolites and nine microbial genera were identified as potential candidates for the biocontrol of *M. incognita*. These findings can provide a better understanding of the environmental changes in the rhizosphere soil of tomatoes infected with *Meloidogyne incognita* and establish a theoretical basis for discovering novel biocontrol agents.

Declaration of Competing Interest

The authors declare that they have no known competing financial interests or personal relationships that could have appeared to influence the work reported in this paper.

Data Availability

Data will be made available on request.

Acknowledgment

References

1. SIKANDAR A., JIA L., WU H., YANG S. *Meloidogyne enterolobii* risk to agriculture, its present status and future prospective for management. Frontiers in Plant Science, **13**, 1093657, **2023**.

2. EL-ASHRY R.M., AIOUB A.A., AWAD S.E. Suppression of *Meloiodogyne incognita* (Tylenchida: Heteroderidae) and *Tylenchulus semipenterans* (Tylenchida: Tylenchulidae) using *Tilapia* fish powder and plant growth promoting rhizobacteria in vivo and in vitro. European Journal of Plant Pathology, **165**, 665, **2023**.

3. CUCIO C., ENGELEN A.H., COSTA R., MUYZER G. Rhizosphere Microbiomes of European Seagrasses are selected by the plant, but are not Species Specific. Frontiers in Microbiology, **7**, 440, **2016**.

4. PHILIPPOT L., RAAIJMAKERS J.M., LEMANCEAU P., VAN DER PUTTEN W.H. Going back to the roots: the microbial ecology of the rhizosphere. Nature Reviews Microbiology, **11** (11), 789, **2013.**

5. HOLMER R., RUTTEN L., KOHLEN W., VAN VELZEN R., GEURTS R. Commonalities in symbiotic plant-microbe signalling. Advances in Botanical Research, **82**, 187, **2017**.

6. HU L., ROBERT C.A.M., CADOT S., ZHANG X., YE M., LI B. Root exudate metabolites drive plant-soil feedbacks on growth and defense by shaping the rhizosphere microbiota. Nature Communications, **9**, 2738, **2018**.

7. VOGES M., BAI Y., SCHULZE-LEFERT P., SATTELY E.S. Plant-derived coumarins shape the composition of an Arabidopsis synthetic root microbiome. Proceedings of the National Academy of Sciences of the United States of America, **116** (25), 12558, **2019**

8. FINKEL O.M., SALAS-GONZÁLEZ I., CASTRILLO G., CONWAY J.M., LAW T.F., TEIXEIRA P.J.P.L. A single bacterial genus maintains root growth in a complex microbiome. Nature, **587** (5832), 103, **2020**.

9. PANG Z., CHEN J., WANG T., GAO C., LI Z., GUO L., XU J., CHENG Y. Linking Plant Secondary Metabolites and Plant Microbiomes: A Review. Frontiers in Plant Science, **12**, 621276, **2021**.

10. ALI A.A., EL-ASHRY R.M., AIOUB A.A. Animal manure rhizobacteria cofertilization suppresses phytonematodes and enhances plant production: Evidence from field and greenhouse. Journal of Plant Diseases and Protection, **129** (1), 171, **2021**.

11. FENG Y., RUI L., WANG X., WU X. Adaptation of pine wood nematode, *Bursaphelenchus xylophilus*, early in its interaction with two *Pinus* species that differ in resistance. Journal of Forestry Research, **33** (4), 1391, **2022**.

12. ZHAO X., LIN C., TAN J., YANG P., WANG R., QI G. Changes of rhizosphere microbiome and metabolites in *Meloidogyne incognita* infested soil. Plant and Soil, **483** (1-2), 331, **2023**.

13. TONG W., LI J., CONG W., ZHANG C., XU Z., CHEN X., YANG M., LIU J., YU L., DENG X. Bacterial Community Structure and Function Shift in Rhizosphere Soil of Tobacco Plants Infected by *Meloidogyne incognita*. Plant Pathology Journal, **38** (6), 583, **2022**.

14. STEEL R., TORRIE J. Principles and procedures of statistics: A biometrical approach MCGraw-Hill Book Company Toronto. Redvet, **13** (6), 481, **2012.**

15. KIRIENKO D.R., REVTOVICH A.V., KIRIENKO N.V. A High-Content, Phenotypic Screen Identifies Fluorouridine as an Inhibitor of Pyoverdine Biosynthesis and *Pseudomonas aeruginosa* Virulence. Msphere, **1**, **2017**.

16. HUANG C.Y., CHEN Y.C., WU-HSIEH B.A., FANG J.M., CHANG Z.F. The Ca-loop in thymidylate kinase is critical for growth and contributes to pyrimidine drug sensitivity of *Candida albicans*. Journal of Biological Chemistry, **294** (27), 10686, **2019**.

17. DREAU D., FOSTER M., HOGG M., CULBERSON C., NUNES P., WUTHIER R.E. Inhibitory effects of fusarochromanone on melanoma growth. Anti-Cancer Drugs, **18**, 897, **2007**.

18. ABDEL-RAHMAN A.A., KESBA H.H., AL-SAYED A.A. Activity and reproductive capability of Meloidogyne incognita and sunflower growth response as influenced by root exudates of some medicinal plants. Biocatalysis and Agricultural Biotechnology, **22**, **2020**.

19. PIETERSE C.M.J., ZAMIOUDIS C., BERENDSEN R.L., WELLER D.M., VAN WEES S.C.M., BAKKER P.A.H.M. Induced systemic resistance by beneficial microbes. Annual Review of Phytopathology, **52**, 347, **2014**.

20. REINHOLD-HUREK B., BUNGER W., BURBANO C.S., SABALE M., HUREK T. Roots shaping their microbiome: global hotspots for microbial activity. Annual Review of Phytopathology, **53**, 403, **2015**

21. GOUDA S., KERRY R.G., DAS G., PARAMITHIOTIS S., SHIN H.S., PATRA JK. Revitalization of plant growth promoting rhizobacteria for sustainable development in agriculture. Microbiological Research, **206**, 131, **2017**.

22. LUO T., HOU S.S., YANG L., QI G.F., ZHAO X.Y. Nematodes avoid and are killed by *Bacillus mycoides*-produced styrene. Journal of Invertebrate Pathology, **159**, 129, **2018**.

23. LAMY E., PATUREL C., WINKLER T. Synthesis and reactivity of 4 phenylsul fonamide avermectin B1 and 4 Phenylsul finimineavermectin B1 monosaccharide derivative. Tetrahedron Letters, **47**, 5657, **2006**.

24. QURESHI S.A., RUQQIA SULTANA V., ARA J., EHTESHAMUL-HAQUE S. Nematicidal potential of culture filtrates of soil fungi associated with rhizosphere and rhizoplane of cultivated and wild plants. Pakistan Journal of Botany, **44** (3), 1041, **2012**.

25. PERSHINA E.V., IVANOVA E.A., NAGIEVA A.G., ZHIENGALIEV A.T., CHIRAK E.L., ANDRONOV E.E., SERGALIEV N.K. A Comparative Analysis of Microbiomes in Natural and Anthropogenically Disturbed Soils of Northwestern Kazakhstan. Eurasian Soil Science, **49** (6), 673, **2016**.

26. FUDOU R., JOJIMA Y., IIZUKA T., YAMANAKA S. *Haliangium ochraceum* gen. nov., sp. nov. and *Haliangium tepidum* sp. nov.: novel moderately halophilic myxobacteria isolated from coastal saline environments. The Journal of General and Applied Microbiology, **48** (2), 109, **2020**.

27. JANG J.H., KIM M.K., SATHIYARAJ S., LEE J., JUYOUNG K., MAENG S., LEE K.E., LEE E.Y., KANG M.S., SATHIYARAJ G. A report of eight unrecorded radiation resistant bacterial species in Korea isolated in 2018. Journal of Species Research, **7** (3), 210, **2018**.

28. ZHENG Z.G., ZHENG J.S., LIU H.L., PENG D.H., SUN M. Complete genome sequence of *Fictibacillus phosphorivorans* G25-29, a strain toxic to nematodes. Journal of Biotechnology, **239**, 20, **2016**.

29. LIU M., XING S.S., YUAN W.D., WEI H., SUN Q.G., LIN X.Z., HUANG H.Q., BAO S.X. *Pseudonocardia nematodicida* sp nov., isolated from mangrove sediment in Hainan, China. Antonie Van Leeuwenhoek International Journal of General and Molecular Microbiology, **108** (3), 571, **2015**.

30. DE MENEZES C.B.A., TONIN M.F., SILVA L.J., DE SOUZA W.R., PARMA M., DE MELO L.S., ZUCCHI T.D., DESTEFANO S.A.L., FANTINATTI-GARBOGGINI F. *Marmoricola aquaticus* sp nov., an actinomycete isolated from a marine sponge. International Journal of Systematic and Evolutionary Microbiology, **65**, 2286, **2015**.

31. LEE S.D., LEE D.W., KO Y.H. *Marmoricola korecus* sp nov. International Journal of Systematic and Evolutionary Microbiology, **61**, 1628, **2011**.